AIChE

Self-Assembly of Novel Architectural Nanohybrid Multilayers and their Selective Separation of Solvent-Water Mixtures

Guojun Zhang, Jie Li, and Shulan Ji
Center for Membrane Technology, College of Environmental and Energy Engineering, Beijing University of Technology, Beijing, 100124, China

DOI 10.1002/aic.12697
Published online June 24, 2011 in Wiley Online Library (wileyonlinelibrary.com).

A new architectural nanohybrid multilayer has been explored and built on various substrates. The building blocks of positive and negative charged polyelectrolyte-coated nanoparticles (NPs) could be obtained by tuning the electrical properties of the amphoteric oxide NPs in acid and basic environments. The nanohybrid films were, thereafter, formed by layer-by-layer (LbL) assembly of polycation- and polyanion-coated NPs. It was demonstrated that this approach could incorporate single component NPs into both polycation and polyanion layers, and in turn improve the NP loading, maintain good dispersion of NPs within the film. For separation applications, a dynamic LbL assembly was attempted as a means of fabricating such nanohybrid multilayers on both 2-D and 3-D polymeric porous substrates. The nanohybrid multilayer membrane renders both much higher selectivity and flux in the separation of solvent-water mixtures. Moreover, such assembly of nanohybrid multilayers allows us to efficiently simplify the procedures by reducing 30–40-fold process cycles. © 2011 American Institute of Chemical Engineers *AIChE J*, 58: 1456–1464, 2012
Keywords: nanohybrid multilayer, nanoparticles, dynamic layer-by-layer assembly, hollow fiber, pervaporation

Introduction

In recent years, the construction of inorganic/organic nanohybrid films on solid substrate surfaces with nanometer-control over their properties have received considerable interest due to their potential and/or demonstrated applications such as microcapsules,[1] fuel cell,[2] sensitive solar cell films,[3] biosensors[4,5] and separation membranes.[6–12] Currently, the synthesis of novel architectural nanohybrid films and the development of new fabrication methods for such films, are still the major research goals in this filed. The control of the dispersion of the nanoparticles (NPs) on a chemically diverse range of supports and the loading of NPs in the polymer matrix constitute the fundamental and central problems. In most of the studies, the NPs are synthesized *in situ*, and it is difficult to control the size distribution and dispersion on the supports. Since monodispersive NPs can nowadays be routinely synthesized, many researchers are trying to directly fabricate NP-containing composites by using monodispersive NPs.[13] The versatile layer-by-layer (LbL) self-assembly is considered to be an attractive approach for developing nanostructured supramolecular systems.[14–16] It has been demonstrated that LbL technique can create many advanced nanocomposites with exceptional properties. For instance, He et al.[17] have successfully fabricated polyion/TiO_2 nanocomposite multilayered films by the electrostatic LbL approach, which were subsequently used as working electrodes for dye-sensitized solar cell. Han et al.[18] reported that a

Correspondence concerning this article should be addressed to G. Zhang at zhanggj@bjut.edu.cn.

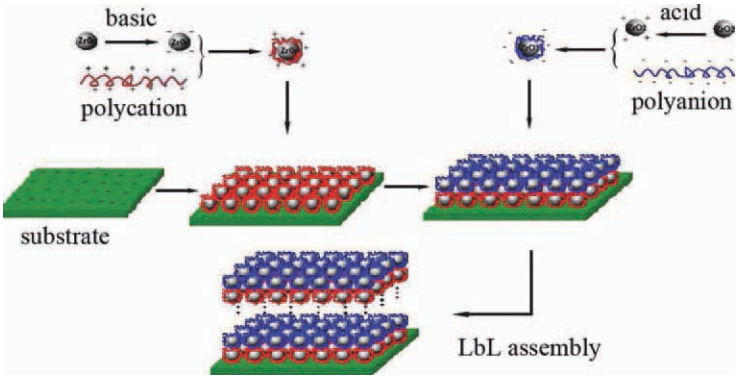

Figure 1. Illustration of proposed constructed nanostructure of polycation-/polyanion-coated NPs multilayer films.

[Color figure can be viewed in the online issue, which is available at wileyonlinelibrary.com.]

superhydrophobic surface can be achieved by a simple LbL procedure of about 10 deposition cycles of poly(allylamine hydrochloride) (PAH) and poly(acrylic acid) (PAA)-coated ZrO_2 NPs and deposition of 1.5 bilayers of PAH and silica NPs, followed by a simple fluorination. Kang et al.[19] have fabricated organic/inorganic hybrid multilayer films with noncentrosymmetrically orientated azobenzene chromophores by the sequential deposition of ZrO_2 layers by a surface sol–gel process and subsequent LbL adsorption of the nonlinear optical (NLO)-active azobenzene-containing polyanion PAC-azoBNS and poly-(diallyldimethylammonium chloride) (PDDA). Hammond and her coworkers have recently created conformal polycation/TiO_2 NP coating on the exterior of the fibers by utilizing a spray LbL technique. The conformal polycation/TiO_2 NP films provide a high-surface area of TiO_2, which is attractive for photocatalysis.[20] Although, there is increasing development of the LbL nanocomposites, previous studies only load NPs into either polycation or polyanion layer. Thus, the NPs loading in nanocomposites are usually limited. Creating new supramolecular NPs hybrid structures to improve the loading of NPs remains one of the most challenging tasks. Furthermore, the selective separation properties of LbL-assembled nanohybrids multilayer remain largely unexplored. Therefore, it is necessary to seek for a new approach to assemble nanohybrid multilayer onto porous substrate and understand the effects of NPs on selective separation process.

Herein, we report on a novel method to construct new architectural nanohybrid films using a facile amphoteric oxide NPs-controlled LbL assembly. The positive and negative charged polyelectrolyte (PE) coated NPs could be formed by adjusting the charge property of the amphoteric oxide NPs in acid and basic environments. The polycation- and polyanion-coated NPs were thereafter used as building blocks for the LbL assembly of nanohybrid multilayer (Figure 1). The growth, film thickness, nanostructure and morphology were systematically investigated by UV–vis spectroscopy, profilometer, SAXRD, SEM, and AFM by assembling nanohybrid multilayers on quartz slides. Subsequently, we extended the assembly of the nanohybrid multilayer to both 2-D flat sheet and 3-D hollow fiber polymeric porous substrates by using a dynamic pressure-driven LbL technique. The resulting nanohybrid multilayer membranes were used as candidates for the pervaporation separation of various solvent-water mixtures.

Experimental Section

Materials

5 wt % aqueous dispersion of ZrO_2 NPs, (particle size $<$100 nm), poly(sodium styrene sulfonate) (PSSNa; M_w 70,000), and PDDA (M_w 100,000–200,000) were purchased from Aldrich. Sodium hydroxide, ethyl acetate, *tert*-butanol, *iso*-butanol, butanol, 2-propanol, ethanol, hydrogen peroxide, and sulfuric acid were provided by Beijing Chemical Factory. Quartz substrates for UV–vis measurements were purchased from Beijing Kinglass Quartz Co., Ltd. The flat sheet polyacrylonitrile (PAN) ultrafiltration (UF) membranes with a nominal molecular weight cutoff of 30,000–40,000 were supplied by Sepro Membranes Inc. Hollow fiber PAN substrate membranes were spun by a dry/wet-phase inversion method in our workshop.[21] The inner diameter of each hollow fiber was 1.1 mm.

Preparation of polyelectrolyte-coated ZrO_2 NPs

To obtain PSS-coated ZrO_2 NPs for subsequent assembly, 8.0 mL of ZrO_2 colloid dispersion (5 wt %) was added to 1.2 wt % PSS solution. The pH value was maintained at 6.0. The mixed solution was sonicated for 30 min. The dispersion was then centrifuged for 10 min at 10,000 rpm. To remove the excess free PSS chains on the surface of NPs, the supernatant was removed and washed with ultrapure water three times. The preliminary PSS-coated ZrO_2 colloid was redispersed by sonication for 30 min and followed by the same procedure of centrifugation and supernatant exchange. Finally, the stable PSS-coated ZrO_2 NPs suspension was obtained after three times of sonication dispersion. The preparation of PDDA-coated ZrO_2 NPs is almost identical with the process of PSS-coated ZrO_2 NPs. 8.0 mL of ZrO_2 colloid dispersion (5 wt %) was mixed with 0.94 wt % PDDA solution. The pH value was adjusted to about 12.0. Then the sonication, centrifugation, and supernatant exchange procedures were sequentially repeated for three times.

Nanohybrid multilayer buildup onto quartz slides

Quartz slides were treated with boiling piranha solution (30:70 v/v H_2O_2: H_2SO_4) for 5 h, followed by rinsing with copious amount of ultrapure water. LbL assembly was

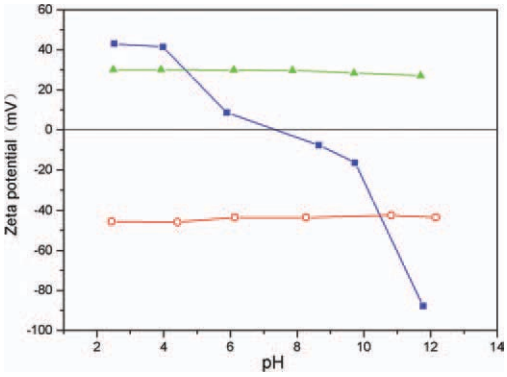

Figure 2. Zeta-potential plots of ZrO_2 (square), PDDA-coated ZrO_2 (triangle), and PSS-coated ZrO_2 (circle) suspensions.

[Color figure can be viewed in the online issue, which is available at wileyonlinelibrary.com.]

performed by sequentially exposing the substrates to PDDA- and PSS-coated ZrO_2 aqueous dispersions for 30 min. Before the next cycle, the films were extensively rinsed with ultrapure water and dried with a nitrogen flow. Alternating PDDA-ZrO_2/PSS-ZrO_2 multilayer films could be obtained by repeating these steps in a cyclic fashion. Control experiments were also conducted by replacing either one or two PE-coated ZrO_2 aqueous dispersion with the corresponding PE aqueous solution during the LbL assembly process. The PDDA-ZrO_2/PSS, PDDA/PSS-ZrO_2 and PDDA/PSS multilayer films could, thereafter, be obtained.

Nanohybrid multilayer buildup onto flat sheet hydrolyzed PAN porous substrates

In the subsequent experiments, we extended the self-assembly of nanohybrid multilayers onto the negatively charged hydrolyzed PAN flat sheet porous substrates. Prior to the assembly, the PAN UF membrane was hydrolyzed for 30 min at 65°C by immersing into a 2 mol/L NaOH aqueous solution.[10] The hydrolyzed membranes were rinsed with ultrapure water and then loaded in a dead-end filtration cell. The nanohybrid multilayers were constructed by dynamically alternatively filtration of oppositely charged PDDA-coated ZrO_2 and PSS-coated ZrO_2 NPs dispersions. The dynamic pressure was maintained at 0.1 MPa, and the assembly time was maintained at 30 min. After each assembly step, the membrane was taken out, rinsed with copious ultrapure water and dried in an oven at 45°C for about 2 h.

Nanohybrid multilayer buildup onto 3-D hollow fiber hydrolyzed PAN porous substrates

The nanohybrid multilayer was also constructed onto a 3-D hollow fiber substrate. Similarly, the negatively charged PAN hollow fibers were first obtained by hydrolyzing with a NaOH aqueous solution. The charged fibers were then put into a polymethylmethcrylate tube with a diameter of 1.5 cm. Both ends of the hollow fiber module were sealed with epoxy resin. The assembly experiments were carried out by using a laboratory fabricated cross-flow negative pressure filtration cell, which has been previously reported.[9] The PDDA-coated ZrO_2 and PSS-coated ZrO_2 NPs dispersions were alternatively provided into the lumen side of hollow fiber and then recycled by using two peristaltic pumps and through separate tubings. On the outer surface side, a vacuum pump was used to form a negative pressure of −0.09 MPa. After each assembly, inner surface of the hollow fiber was rinsed with substantial ultrapure water and dried by recycling filtered nitrogen gas.

Pervaporation experiments

Both flat sheet and hollow fiber nanohybrid multilayer membranes were evaluated by pervaporation separation of 95 wt % solvent-water mixture. The measurement systems have been described in our previous studies.[7–10] However, a specially designed cross-flow system was used to evaluate the hollow fiber nanohybrid multilayer membrane performance.[7-9] The feeding solution contacted with the inner surfaces of the hollow fiber modules. Three modules with same assembly conditions were examined at each pervaporation

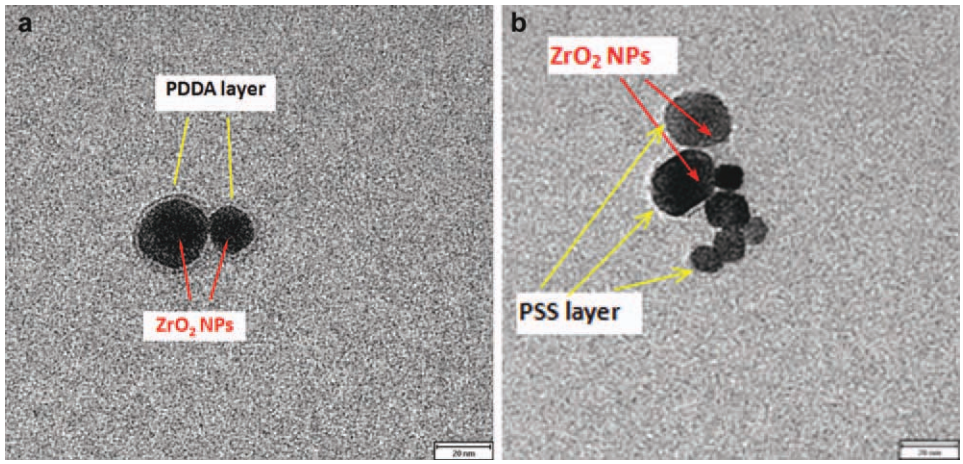

Figure 3. TEM images of the (a) PDDA-coated ZrO_2 nanoparticles at the pH of 12.0, and (b) PSS- coated ZrO_2 nanoparticles at the pH of 6.0.

[Color figure can be viewed in the online issue, which is available at wileyonlinelibrary.com.]

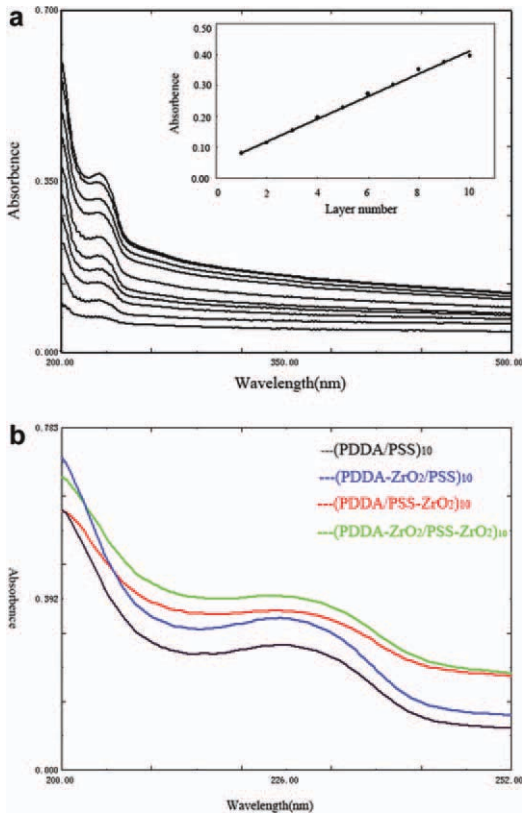

Figure 4. (a) UV–vis spectra of (PDDA-ZrO_2/PSS-ZrO_2) n films with n = 1–10 on quartz substrates (from the bottom to the top).

The inset shows the plots of the absorbance values at 226 nm vs. the number of bilayers, and (b) UV–vis absorption spectra of $(PDDA/PSS)_{10}$, $(PDDA\text{-}ZrO_2/PSS)_{10}$, $(PDDA/PSS\text{-}ZrO_2)_{10}$, and $(PDDA\text{-}ZrO_2/PSS\text{-}ZrO_2)_{10}$ multilayer films assembled on quartz slides from the bottom to the top. [Color figure can be viewed in the online issue, which is available at wileyonlinelibrary.com.]

condition. The permeate vapor was trapped with liquid nitrogen. The down-stream pressure was about 100 Pa. Fluxes were determined by measuring the weight of liquid collected in the cold traps during a certain time under steady-state conditions. The compositions of feeding solutions and permeates were determined with a gas chromatography (GC-14C, SHIMADZU). The separation factor α was calculated from the quotient of the weight ratio of component i and component j in the permeate Y_i/Y_j, and in the feed X_i/X_j.

$$\alpha = \frac{Y_i X_j}{Y_j X_i}$$

Characterization

The zeta potentials of ZrO_2 and PE-coated ZrO_2 NPs were determined by zeta potential analyzer (Zatasizer 200, Malven Co.). Zeta potentials of the hollow fiber inner surfaces were determined using an electrokinetic analyzer (Anton Paar, SurPASS). In the process for measuring the zeta potential, the KCl solution concentration was maintained at 1.0 mol/L, while the operation pressure was 0.03 MPa. The growth of nanohybrid multilayers on quartz slides were monitored using a spectrophotometer (UV-2550, Shimadzu). Film thickness was measured using a XP-1 profilometer (Ambios, USA). A groove in the film was made using a razor blade, and the film thickness was estimated by the depth of the groove measured by profilometer stylus. The thickness was recorded three times at different locations and averaged to yield one data point. Transmission electron microscopy (TEM) measurements were carried out on a JEM-2010 microscopy (JEOL, Ltd., Japan). Samples were prepared by dropping a suspension onto Formvar-coated copper grids. A scanning electron microscopy (SEM) (Hitachi-4700, Japan) was used to observe the multilayer morphologies assembled on different substrates. Small-angle X-ray diffraction experiments were conducted on an X-ray diffractometer (D8 ADVANCE, Bruker/AXS, Germany). Atomic force microscopy (AFM) images were taken in tapping mode by a AFM (Pico Scan^{TM} 2500, USA).

Results and Discussion

It is well recognized that nanoscale dispersion is critical for understanding the potential benefits of incorporating NPs in coatings. In this study, ZrO_2 NPs were used as typical amphoteric oxide NPs. Since the electrical property of NPs plays a rather important role in determining the stability of a suspension, the zeta potentials of ZrO_2, PDDA-coated ZrO_2 and PSS-coated ZrO_2 NPs were measured under different pH values. As shown in Figure 2, the nano-ZrO_2 particles were positively charged in the acidic region. The charge property of nano-ZrO_2 particles could change inversely and become negatively charged in the basic region. Therefore, in this study, it is anticipated that the negatively charged polyanion and positively charged polycation could be successfully coated onto the ZrO_2 NPs under acid and basic conditions, respectively. Prior to assembly, ZrO_2 NPs were dispersed into both PSS and PDDA solutions so as to form two classes of oppositely charged PE-coated ZrO_2 NPs at the pH of 6 and 12, respectively. It is noted that the charges of PDDA-ZrO_2 and PSS-ZrO_2 NPs remained almost constant because the pH value has insignificant effects on the strong polyelectrolytes. Therefore, both PDDA-ZrO_2 and PSS-ZrO_2 NPs were able to remain stabilized and well dispersed into the solution due to the electrostatic repulsion originating from the outer PE layers. Moreover, it was observed from TEM pictures that there were very thin PE layers around ZrO_2 NPs for both PSS- and PDDA-coated NPs (Figure 3). This provided further evidence that the nanohybrid structure could be successfully formed by coating amphoteric oxide NPs with both polycation and polyanion under different pH values.

The LbL self-assembly is considered to be one of the most powerful techniques for tailoring nanostructured thin films. The novel architectural nanohybrid multilayer films were formed on the quartz slides by sequential adsorption of PDDA- and PSS-coated ZrO_2 NPs. The growth of the nanohybrid films with the bilayer numbers was observed by UV–vis spectroscopy (Figure 4a). The increases in the absorbance at 226 nm, which corresponds to aromatic group of PSS, indicated a progressive and uniform deposition process of the (PSS-ZrO_2/PDDA-ZrO_2) n multilayer, and suggested the amounts of adsorbed PDDA- and PSS-coated ZrO_2 NPs in

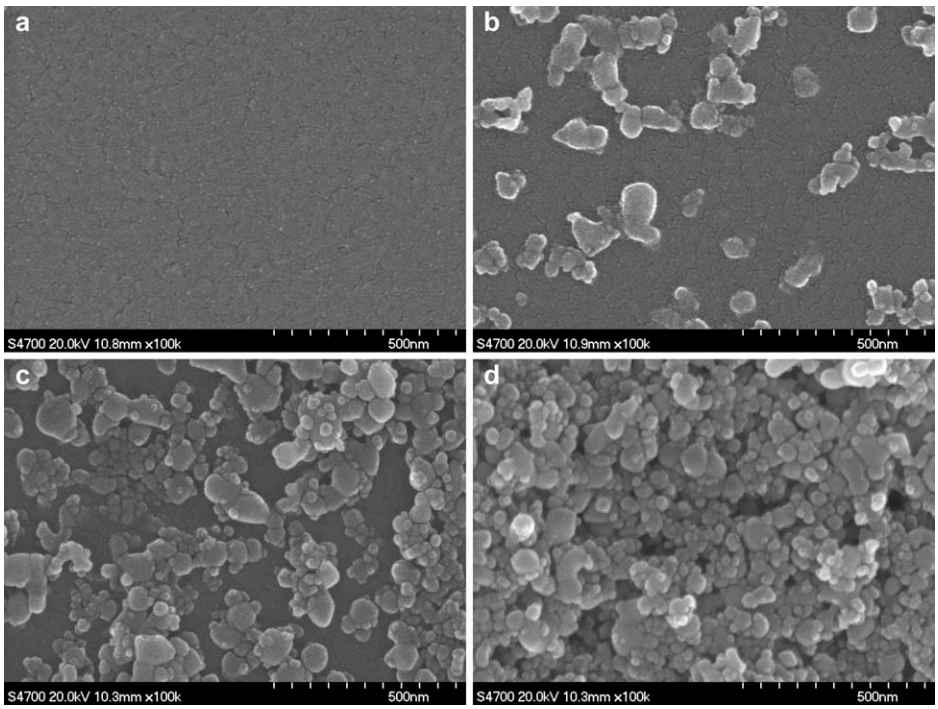

Figure 5. SEM images of (a) PDDA/(PSS/PDDA)$_{10}$ multilayer, (b) PDDA-ZrO_2/(PSS/PDDA-ZrO_2)$_{10}$ multilayer, (c) PDDA/(PSS-ZrO_2/PDDA)$_{10}$ multilayer, and (d) PDDA-ZrO_2/(PSS-ZrO_2/PDDA-ZrO_2)$_{10}$ multilayer.

the assembly process are essentially the same for each layer. Control experiments were conducted on the other two classes of nanohybrid multilayers with ZrO_2 NPs in single PE layer, and PSS/PDDA multilayer without ZrO_2 NPs. The UV–vis spectra also indicated that the nanohybrids embedded into polycation and/or polyanion were beneficial for the film growth (Figure 4b). The film thickness was further characterized by profilometer. The average bilayer thickness of the PSS-ZrO_2/PDDA-ZrO_2 nanohybrid multilayer is approximately 4.1 nm. As a reference, the average bilayer thickness of 3.0 nm was calculated for PSS/PDDA film without ZrO_2 NPs. These results further suggest that the use of nanohybrids for assembly could greatly enhance the film growth and film thickness.

The morphology of multilayer films was examined by SEM. The homogeneous film was formed by the PDDA/(PSS/PDDA)$_{10}$ multilayers (Figure 5a). It was noted from Figure 5b and c that ZrO_2 NPs could be flexibly incorporated into either polyanion or polycation layers by tuning the charge properties. However, the loading of NPs was limited since NPs was only introduced into a single PE layer. As a comparison, a high content of NPs was loaded with little aggregation in the thin film even after alternatively depositing 11 PDDA-ZrO_2 layers and 10 PSS-ZrO_2 layers (Figure 5d). This is caused by the nanostructured incorporation based on the suitable matching of electrostatic attraction between PDDA-ZrO_2 and PSS-ZrO_2 NPs. Simultaneously, the steric hindrance of the outer PE layer was able to avoid hard aggregation among the opposite charged PE-coated NPs, which ensured a satisfactory dispersion of NPs within the LbL assembled multilayer. As shown in Figure 5d, the sizes of PE-coated NPs in the film were predominantly maintained at less than 50 nm. The topography and the surface roughness of multilayer films were also evaluated with AFM. The surface roughness's over 50 $\times$ 50 μm are approximately 16.6 and 163.0 nm for the non-nanohybrid PSS/PDDA and nanohybrid PSS-ZrO_2/PDDA-ZrO_2 films, respectively (Figure 6). Obviously, the film surface becomes much rougher after being embedded with nano-ZrO_2 particles. The small-angle X-ray diffraction data further suggested that the diffraction peaks obtained from PSS-ZrO_2/PDDA-ZrO_2 multilayer were less than those from PSS/PDDA, PSS-ZrO_2/PDDA and PDDA- PSS/PDDA-ZrO_2 multilayers, which indicated that the nanohybrid multilayer became more interpenetrated and much denser after embedding NPs into both the polycation and polyanion layers (Figure 7).

Planar nonporous quartz substrates are readily coated by LbL technique. The assemblies of nanohybrid multilayer onto 2-D flat sheet and 3-D hollow fiber porous substrates remain largely unexplored. Therefore, PE muiltilayers containing high loading NPs assembled onto polymeric porous substrates were subsequently investigated as candidates for separation membranes. Differing from the nonporous rigid substrates, in terms of the unique features of polymeric porous substrates such as wide pore diameter distribution and good permeability, dynamic pressure-driven LbL assembly had recently been developed in our laboratory.[7–10] By drawing a transmembrane pressure across the porous substrates, the nanohybrid multilayers were formed on both 2-D flat sheet and 3-D hollow fiber hydrolyzed PAN UF substrates by alternatively filtrating the polycation- and polyanion-coated NPs solutions. The growth of the self-assembled nanohybrid multilayers onto hollow fibers was tracked via inner surface charge monitoring. The inner surface zeta potential as a function of the number of nanohybrid layers deposited is shown in Figure 8. In Figure 8, the odd and even layer numbers correspond to the PDDA-ZrO_2 and PSS-

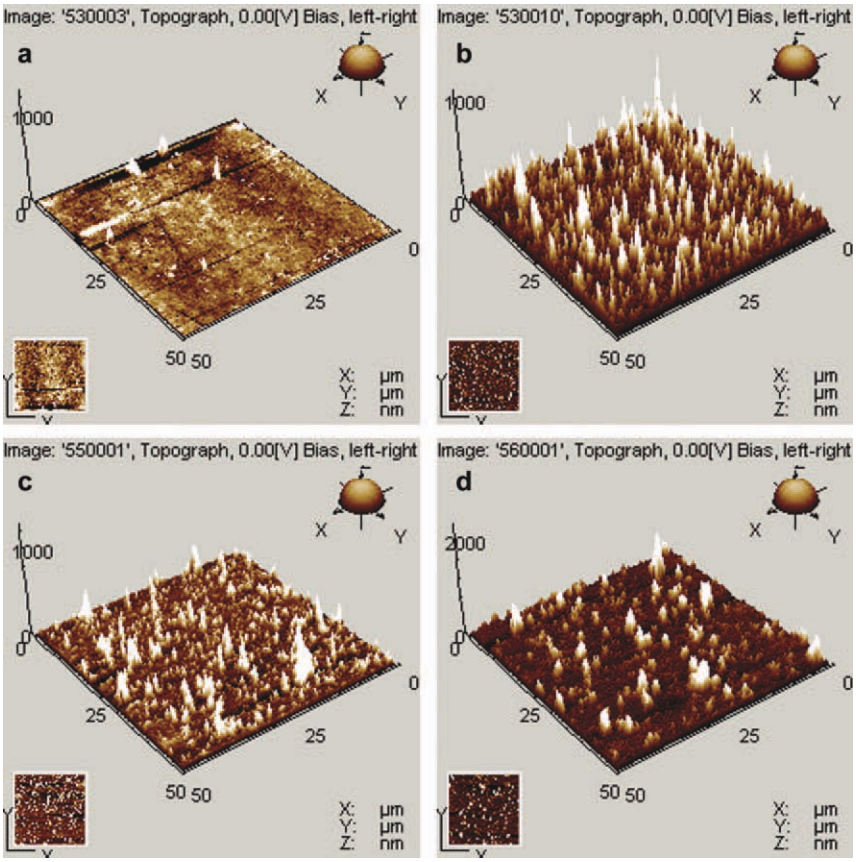

Figure 6. Tapping mode 3-D AFM images of multilayer films (50.0 μm × 50.0 μm).

(a) PDDA/(PSS/PDDA)$_{10}$, (Ra = 16.6 nm), (b) PDDA/(PSS-ZrO_2/PDDA)$_{10}$, (Ra = 134 nm), (c) PDDA-ZrO_2/(PSS/PDDA-ZrO_2)$_{10}$, (Ra = 70.7 nm), and (d) PDDA-ZrO_2/(PSS-ZrO_2/PDDA-ZrO_2)$_{10}$, (Ra = 163 nm). [Color figure can be viewed in the online issue, which is available at wileyonlinelibrary.com.]

ZrO_2 adsorption steps, respectively. It was noted that the hydrolyzed PAN substrate was negatively charged because the –CN groups changed into carboxylate groups during the alkaline hydrolysis process. The charge property of inner surface can change inversely and become positively charged after assembling one PDDA-ZrO_2 layer. As serial deposition continued, the zeta potential of inner surface almost regularly alternated between +6 mV and −6 mV when PDDA-ZrO_2 and PSS-ZrO_2 formed the outer layers, respectively. Such alternating reversals in the sign of the zeta potential are characteristic for the LbL formation of multilayers on hollow fibers, suggesting stepwise nanohybrid layer growth of PDDA-ZrO_2 and PSS-ZrO_2 on the inner surface of hydrolyzed PAN hollow fibers.

In recent years, the construction of various multilayers onto porous substrates appears to be an efficient way to create unique property for separation purposes such as pervaporation, gas separation and desalination. Particularly, pervaporation dehydration has drawn much attention because solvent dehydration is a difficult problem in many cases such as fuel ethanol production, pharmaceutical and petrochemical manufactures. In fact, pervaporation is a promising and spreading membrane technology in chemical process industries due to its low-energy requirements and its simplicity when compared to conventional separation techniques.[22–25] Therefore, the resulting nanohybrid multilayer membranes were used for pervaporation separation of solvent-water mixtures. All the pervaporation studies done with ethanol-water mixtures have shown that the membrane performance is strongly affected by the NPs incorporation (Figure 9). It is well-known that there is a trade-off between permeability and selectivity for dense pervaporation membranes. Generally, the increase of selectivity leads to the decrease of permeability. Interestingly, the experimental results in Figure 9 showed a trend that the incorporation of ZrO_2 NPs into both polycation and polyanion layers appeared to possess both much higher selectivity and flux. For example, in the case of separation of ethanol-water mixture using hollow fiber PSS-ZrO_2/PDDA-ZrO_2 nanohybrid membrane, the water content could be enriched from 5.0 wt % (in feed) to 99.9 wt % (in permeate), which meant that the separation factor (α) could reach 18981, while the permeate flux was 340 g/(m^2.h) (50°C), respectively. The greater enhancement on the separation properties of PSS-ZrO_2/PDDA-ZrO_2 nanohybrid membranes in comparison with the PSS/PDDA, PSS-ZrO_2/PDDA and PSS/PDDA-ZrO_2 is generally attributable to better structured nanocomposites. The same trend is also observed with the flat sheet nanohybrid multilayer membranes. The

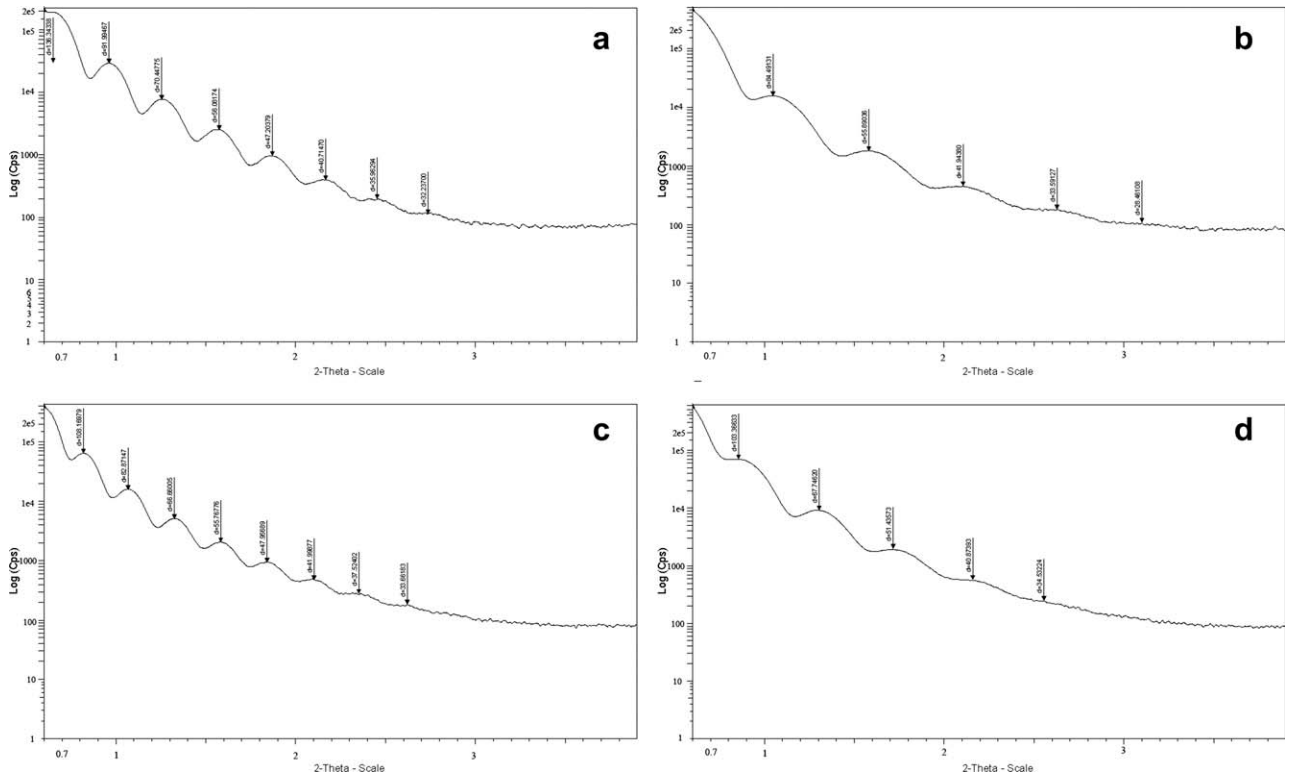

Figure 7. Small-angle X-ray diffraction pattern of (a) PDDA/(PSS/PDDA)$_{10}$ multilayer, (b) PDDA/(PSS-ZrO$_2$/PDDA)$_{10}$ multilayer, (c) PDDA-ZrO$_2$/(PSS/PDDA-ZrO$_2$)$_{10}$ multilayer, and (d) PDDA-ZrO$_2$/(PSS-ZrO$_2$/PDDA-ZrO$_2$)$_{10}$ multilayer films on quartz substrates.

performance of nanohybird membranes is closely related to their structure. When the inorganic NPs are embedded in organic matrices, these NPs modify transport properties without introducing gross defects into the membrane. The molecules must diffuse along the surface of PE-coated NPs and pass through the polymeric matrix among the NPs. The diffusion path is, therefore, changed and prolonged, which leads to the increase in diffusion selectivity. The NPs act so as to create preferential permeation pathways for selective permeation while imposing a barrier for undesired permeation. Moreover, the rougher surface provides a much larger contact area between feed solution and membrane surface. Meanwhile, the improvement of the flow status due to the rougher nanostructure is also helpful to alleviate the concentration polarization near the selective layer. These result in a higher flux. It was also noted from Figure 9 that the hollow fibers performed better than the flat sheets in terms of water content in permeate. The similar trend is also observed in the assembly of polyelectrolyte complex membrane.[26] This is due to the different structure of hollow fiber and flat sheet. Because hollow fiber is a self-contained mechanical support while flat sheet membrane contained nonwoven substrate, the membrane pore of hollow fibers might shrink much more flexibly and easily during the alkaline hydrolysis process. The complex membrane would then become much denser and in turn would have higher selectivity. Accordingly, the fluxes of hollow fibers were much lower than those of flat sheets.

The improved pervaporation separation properties of nanohybrid multilayer membranes were not only restricted to the dewatering of ethanol, but were also observed for other low-molecular-weight organics. The pervaporation performance of flat sheet nanohybrid multilayer membrane was evaluated using different solvent-water mixtures. As can be

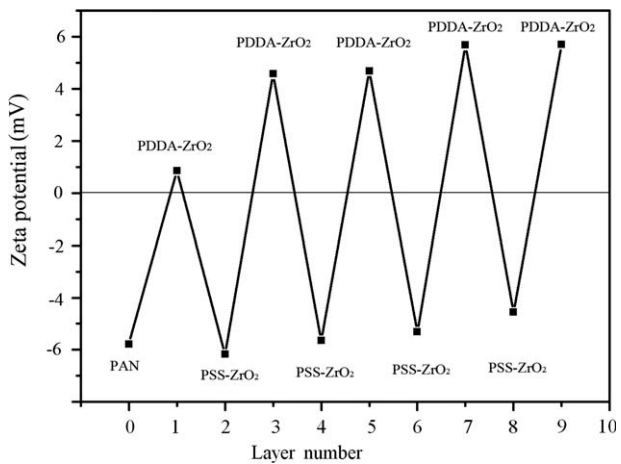

Figure 8. Variations of inner surface zeta potential with layer numbers during the assembly of (PDDA-ZrO$_2$/PSS-ZrO$_2$)n onto hollow fiber PAN substrate membrane.

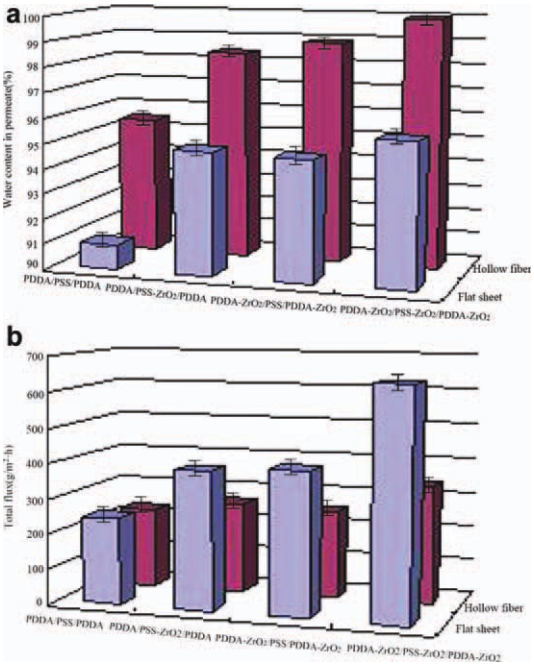

Figure 9. Pervaporation separation of ethanol-water mixture with flat sheet and hollow fiber nanohybrid multilayer membranes (a) water content in the permeate, and (b) total flux (measurement temperature: flat sheet membrane, 60°C; hollow fiber, 50°C).

[Color figure can be viewed in the online issue, which is available at wileyonlinelibrary.com.]

expected from our results (Figure 10), the selectivity toward alcohol-containing water mixtures should increase with alcohol molecular size arising. However, the nanohybrid multilayer membranes also showed excellent pervaporation dehydration performance for 95.0 wt % ethyl acetate-water mixture. The water content in permeate and permeate flux reached 99.7% (α = 6314), and 3426 g/(m^2.h), respectively. It means that nanohybrid multilayers could be a promising candidate for various solvent-water separations. Additionally, one of the most important points was that only two PDDA-ZrO_2 layers plus one PSS-ZrO_2 layer (i.e., 1.5 bilayers) were assembled to achieve such a high performance. Compared to the traditional static LbL assembly, which usually requires as many as 50–60 PE bilayers to obtain defect-free dense membranes,[11,12] the dynamic LbL assembly of both polycation and polyanion nanohybrids allows us to realize 30–40-fold decreases in process cycles. To date, although LbL technique has attached much attention and experimentally explored by scientists from different fields, no important practical application has yet emerged. The main reason is that the LbL process involves numerous deposition and rinsing steps, and this complexity greatly limits the potential applications of multilayer coatings.[27] The high reduction of deposition cycles in this study offers much opportunity for the potential scale-up of LbL-assembled nanohybrid multilayer membranes. Moreover, this technique could be easily extended to various membrane modules, such as flat sheet, tubular and hollow fiber. Taking into account that this approach can be applied, in principle, to other LbL-assembled nanohybrid multilayers, it will open significant possibilities for the rapid construction of new multilayers on various substrates, which will be of considerable use in many separation fields.

Conclusions

In summary, we have developed a simple approach to prepare nanohybrid multilayers on various substrates by using amphoteric oxide NPs-controlled self-assembly. The method provides a general technique to fabricate novel heterostructured nanohybrid thin films containing high loading and well-dispersed NPs. Moreover, it was demonstrated that the assemblies of nanohybrids onto porous substrates for pervaporation separation offered both higher selectivity and higher permeability. Particularly, the dynamic pressure-driven LbL assembly of nanohybrid multilayers allows us to efficiently simplify the procedures by reducing 30–40-fold process cycles. The experiments demonstrate that it is capable of creating nanohybrid coatings onto both 2-D and 3-D substrates. This makes dynamic LbL an attractive technique for scale-up and future development of nanohybrid multilayers for many uses. Currently, further experiments are being carried out to extend this new approach to prepare Al_2O_3 and ZnO nanohybrid multilayers for separation membranes and gas sensors.

Acknowledgments

This work was financially supported by the National Basic Research Program of China (no.2009CB623404), the National Natural Science Foundation of China (no.20806001), and the Scientific Research Common Program of Beijing Municipal Commission of Education (KM201010005016).

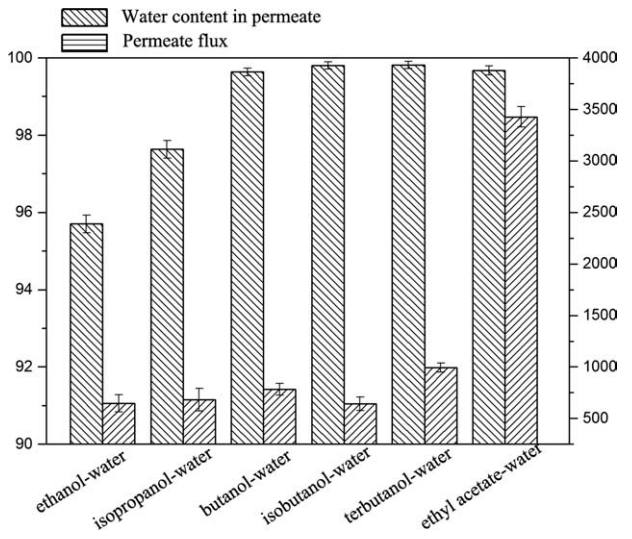

Figure 10. Flat sheet PDDA-ZrO_2/PSS-ZrO_2/PDDA-ZrO_2/PAN membrane performance for the pervaporation separation of 95 wt % solvent solutions at 60°C.

Literature Cited

1. Simovic S, Heard P, Hui H, Song Y, Peddie F, Davey A, Lewis A, Rades T, Prestidge A. Dry hybrid lipid–silica microcapsules engineered from submicron lipid droplets and nanoparticles as a novel delivery system for poorly soluble drugs. *Mol Pharm*. 2009;6(3): 861–872.
2. Lakshminarayana G, Nogami M. Synthesis and characterization of proton conducting inorganic–organic hybrid nanocomposite membranes based on mixed PWA-PMA-TEOS-GPTMS-H_3PO_4-APTES for H_2/O_2 fuel cells. *J Phys Chem C*. 2009;113:14540–14550.
3. Leventis H, King S, Sudlow A, Hill M, Molloy K, Haque S. Nanostructured hybrid polymer–inorganic solar cell active layers formed by controllable in situ growth of semiconducting sulfide networks. *Nano Lett*. 2010;10:1253–1258.
4. Hong W, Bai H, Xu Y, Yao Z, Gu Z, Shi G. Preparation of gold nanoparticle/graphene composites with controlled weight contents and their application in biosensors. *J Phys Chem C*. 2010;114:1822–1826.
5. Li Q, Quinn J, Wang Y, Caruso F. Preparation of nanoporous polyelectrolyte multilayer films via nanoparticle templating. *Chem Mater*. 2006;18:5480–5485.
6. Kim S, Jinschek J, Chen H, Sholl D, Marand E. Scalable fabrication of carbon nanotube/polymer nanocomposite membranes for high flux gas transport. *Nano Lett*., 2007;7:2806–2811.
7. Zhang G, Dai L, Ji S. Dynamic pressure-driven covalent assembly of inner skin hollow fiber multilayer membrane. *AIChE J*. 2010. doi:10.1002/aic.12481.
8. Zhang G, Ruan Z, Ji S, Liu Z. Construction of metal-ligand-coordinated multilayers and their selective separation behavior. *Langmuir*. 2010;26:4782–4789.
9. Zhang G, Wang N, Song X, Ji S, Liu Z. Preparation of pilot-scale inner skin hollow fiber pervaporation membrane module: effects of dynamic assembly conditions. *J Membr Sci*. 2009;338:43–50.
10. Zhang G, Yan H, Ji S, Liu Z. Self-assembly of polyelectrolyte multilayer pervaporation membranes by a dynamic layer-by-layer technique on a hydrolyzed polyacrylonitrile ultrafiltration membrane. *J Membr Sci*. 2007;292:1–8.
11. Krasemann L, Toutianoush A, Tieke B. Self-assembled polyelectrolyte multilayer membranes with highly improved pervaporation separation of ethanol/water mixtures. *J Membr Sci*. 2001;181:221–228.
12. Toutianoush A, Tieke B. Pervaporation separation of alcohol/water mixtures using self-assembled polyelectrolyte multilayer membranes of high charge density. *Mater Sci Eng C*. 2002;22:459–463.
13. Yuan B, Xing L, Zhang Y, Lu Y, Mai Z, Li M. Self-Assembly of highly oriented lamellar nanoparticle-phospholipid nanocomposites on solid surfaces. *J Am Chem Soc*. 2007;129:11332–11333.
14. Lee S, Lee B, Kim B, Park J, Yoo M, Bae W, Char K, Hawker C, Bang J, Cho J. Free-standing nanocomposite multilayers with various length scales, adjustable internal structures, and functionalities. *J Am Chem Soc*. 2009;131:2579–2587.
15. Boudou T, Crouzier T, Ren K, Blin G, Picart C. Multiple functionalities of polyelectrolyte multilayer films: new biomedical applications. *Adv Mater*. 2010;22:441–467.
16. Wang Y, Angelatos A, Caruso F. Template synthesis of nanostructured materials via layer-by-layer assembly. *Chem Mater*. 2008;20: 848–858.
17. He J, Mosurkal R, Samuelson L, Li L, Kumar J. Dye-sensitized solar cell fabricated by electrostatic layer-by-layer assembly of amphoteric TiO_2 nanoparticles. *Langmuir*. 2003;19:2169–2174.
18. Han J, Zheng Y, Cho J, Xu X, Cho K. Stable Superhydrophobic organic–inorganic hybrid films by electrostatic self-assembly. *J Phys Chem B*. 2005;109:20773–20778.
19. Kang E, Bu T, Jin P, Sun J, Yang Y, Shen J. Layer-by-layer deposited organic/inorganic hybrid multilayer films containing noncentrosymmetrically orientated azobenzene chromophores. *Langmuir*. 2007;23:7594–7601.
20. Krogman K, Lowery J, Zacharia N, Rutledge G, Hammond P. Spraying asymmetry into functional membranes layer-by-layer. *Nature Mater*. 2009;8:512–518.
21. Liu Z, Zhang G, Peng Y, Ji S. The hollow fiber ultrafiltration membrane with inner skin and its application. *Desalination*. 2008;233: 55–63.
22. Wang Y, Chung T, Wang H. Polyamide-imide membranes with surface immobilized cyclodextrin for butanol isomer separation via pervaporation. *AIChE J*. 2010. doi:10.1002/aic.12360.
23. Yang D, Li J, Jiang Z, Lu L, Chen X. Chitosan/TiO_2 nanocomposite pervaporation membranes for ethanol dehydration. *Chem Eng Sci*. 2009;64:3130–3137.
24. Ueda Y, Tanaka T, Iizuka A, Sakai Y, Kojima T, Satokawa S, Yamasaki A. Membrane separation of ethanol from mixtures of gasoline and bioethanol with heat-treated PVA membranes. *Ind Eng Chem Res*. 2010. doi:10.1021/ie1014662.
25. Xu J, Gao C, Feng X. Thin-film-composite membranes comprising of self-assembled polyelectrolytes for separation of water from ethylene glycol by pervaporation. *J Membr Sci*. 2010;352:197–204.
26. Zhang G, Gao X, Ji S, Liu Z, One-step dynamic assembly of polyelectrolyte complex membranes, *Mater Sci Eng*. 2009;29:1877–1884.
27. Bruening M, Dotzauer D. Just spray it. *Nature Mater*. 2009;8:449–450.

Manuscript received Jan. 6, 2011, revision received Apr. 5, 2011, and final revision received Jun. 1, 2011.